Article

Ectodermal-neural cortex 1 isoforms have contrasting effects on MC3T3-E1 osteoblast mineralization and gene expression[†]

Running title: *ENC1 isoform effects on MC3T3 differentiation*

Leah E. Worton[1,2*], Yan-Chuan Shi[3,4], Elisabeth J. Smith[3], Simon C. Barry[5], Thomas J. Gonda[1], Jonathan P. Whitehead[6], Edith M. Gardiner[1,2]

[1]The University of Queensland, Brisbane, QLD, Australia
[2]Department of Orthopaedics and Sports Medicine, University of Washington, Seattle, WA, USA
[3]Garvan Institute of Medical Research, Sydney, NSW, Australia
[4]Faculty of Medicine, University of New South Wales, NSW, Australia
[5]The University of Adelaide, Adelaide, SA, Australia
[6]Mater Research Institute, Brisbane, QLD, Australia

* Correspondence to: Dr. Leah E Worton, Department of Orthopaedics and Sports Medicine, Mail stop 359798, 325 Ninth Ave, Seattle, WA, 98104, Telephone: (206) 897-5607; FAX: (206) 897-5611; E-mail: lworton@u.washington.edu

[†]This article has been accepted for publication and undergone full peer review but has not been through the copyediting, typesetting, pagination and proofreading process, which may lead to differences between this version and the Version of Record. Please cite this article as doi: [10.1002/jcb.25851]

Additional Supporting Information may be found in the online version of this article.

ABSTRACT

The importance of Wnt pathway signaling in development of bone has been well established. Here we investigated the role of a known Wnt target, ENC1 (ectodermal-neural cortex 1; NRP/B), in osteoblast differentiation. *Enc1* expression was detected in mouse osteoblasts, chondrocytes and osteocytes by *in situ* hybridization, and osteoblastic expression was verified in differentiating primary cultures and MC3T3-E1 pre-osteoblast cells, with 57kDa and 67kDa ENC1 protein isoforms detected throughout differentiation. Induced knockdown of both ENC1 isoforms reduced alkaline phosphatase staining and virtually abolished MC3T3-E1 mineralization. At culture confluence, *Alpl* (alkaline phosphatase liver/bone/kidney) expression was markedly reduced compared with control cells, and there was significant and coordinated alteration of other genes involved in cellular phosphate biochemistry. In contrast, with 67kDa-selective knockdown mineralized nodule formation was enhanced and there was a 2-fold increase in *Alpl* expression at confluence. There was enhanced expression of Wnt/β-catenin target genes with knockdown of both isoforms at this time-point and a 5-fold increase in *Frzb* (Frizzled related protein) with 67kDa-selective knockdown at mineralization, indicating possible ENC1 interactions with Wnt signaling in osteoblasts. These results are the first to demonstrate a role for ENC1 in the control of osteoblast differentiation. Additionally, the contrasting mineralization phenotypes and transcriptional patterns seen with coordinate knockdown of both ENC1 isoforms vs selective knockdown of 67kDa ENC1 suggest opposing roles for the isoforms in regulation of osteoblastic differentiation, through effects on *Alpl* expression and phosphate cellular biochemistry. This study is the first to report differential roles for the ENC1 isoforms in any cell lineage. This article is protected by copyright. All rights reserved

INTRODUCTION

It is now understood that the Wnt pathway plays an important role in osteoblast differentiation and bone development, and understanding this mechanism will be advantageous as the Wnt pathway becomes a focus for potential anabolic therapeutics [Shah et al., 2015]. *Enc1* is a Wnt target gene [Fujita et al., 2001] implicated in the control of differentiation along several cell lineages [Kim et al., 2009; Kim et al., 1998; Zhao et al., 2000]. For example, reduction of *Enc1* expression by RNA interference inhibited neuronal differentiation *in vitro* [Kim et al., 1998]. Proposed mechanisms for a neuronal ENC1 function include binding to Retinoblastoma protein (RB1), thereby leading to cell cycle withdrawal [Kim et al., 1998], and ENC1 acting as a nuclear matrix protein via actin binding [Liang et al., 2004]. Knockdown of *Enc1* similarly inhibited adipocyte differentiation *in vitro* [Zhao et al., 2000], with actin binding by ENC1 a proposed requisite for cytoskeletal changes during adipocyte maturation.

ENC1 is a member of the BTB-Kelch family, with conserved amino terminal BTB/POZ and carboxy terminal Kelch protein interaction domains [Prag and Adams, 2003] linked by an intervening BACK domain in some family members [Stogios and Prive, 2004]. Some BTB-Kelch proteins are implicated in cellular functions requiring cytoskeletal stability [Ding et al., 2002; Jiang et al., 2005; Robinson and Cooley, 1997]. Several have been found to serve as adapters to target specific substrate proteins for E3 ubiquitin ligase mediated regulation or proteasomal degradation [Angers et al., 2006; Kobayashi et al., 2004; Metzger et al., 2013]. A few family members appear to provide both functions [Kang et al., 2004; Salinas et al., 2006]. Human and mouse ENC1 proteins share 98% amino acid homology [Hernandez et al., 1998]. Two ENC1 protein species of 67kDa and 57kDa were immunologically detected in rat primary neurons and in rat and human neuroblastoma cell lines, with the 67kDa polypeptide attributed to the full length coding region [Kim et al., 1998] and subsequent functional studies of ENC1 focused on this isoform. A shorter amino-terminally truncated isoform of human ENC1 was predicted by bioinformatic analysis [Resch et al., 2004] but, to date, no mouse 57kDa ENC1 homolog has been reported.

Investigations into the molecular details of ENC1 protein function have largely been driven by its BTB-Kelch domain structure. Like other BTB-Kelch proteins full length 67kDa ENC1 has been found to co-localize with cytoplasmic actin [Hernandez et al., 1997; Liang et al., 2004; Zhao et al., 2000], but also to bind *in vitro* to nuclear proteins RB1 [Kim et al., 1998], E2F transcription factor and histone deacetylase 1 (HDAC1) [Choi et al., 2014], and NFE2-related factor 2 (NRF2) [Seng et al., 2010; Seng et al., 2007]. In addition, there is some evidence that ENC1 may act as an E3 ligase substrate adaptor [Zhang et al., 2005], although no specific target protein has yet been identified for this potential role. A recent report also found that ENC1 interacts with p62 in neuronal cells during ER stress [Lee et al., 2016]. Functional attributes of the 57kDa ENC1 isoform have not yet been tested.

Although a specific role for ENC1 in bone cell biology has not previously been investigated, *Enc1* was one of several Wnt related genes in mouse bone that responded to spinal cord injury [Sun et al., 2013]. As ENC1 has been implicated in adipose and neuronal cell differentiation, we investigated the potential involvement of ENC1 in the regulation of osteoblastic differentiation, as well as the possibility that the two protein isoforms might have distinguishable roles in this context.

MATERIALS AND METHODS

In situ hybridization
For riboprobe preparation, a sequence corresponding to nucleotides 777-1264 in the coding region of the human *ENC1* gene (NM_003633) was amplified by RT-PCR from MG63 (RRID:CVCL_0426) cDNA using hEnc1 primers 5'-GCTGGAGTTTCAAGACATCC-3' and 5'-GGGCACAGAGGCTGGTTACC-3' and cloned into pBluescript SK+ (Stratagene). Sense and antisense riboprobes labeled with digoxigenin-uridine triphosphate (Roche Applied Science) were prepared by *in vitro* transcription. *In situ*

hybridization was performed on sections of paraffin embedded decalcified adult mouse distal femur using a modified protocol [Sims et al., 1997]. Sections were permeabilized in 0.3% triton X-100/PBS for 20 min at RT and then incubated with 10ug/ml Proteinase K at 37°C for 15 min. Sections were pre-hybridized at 42°C for 30 min and hybridized with riboprobe (60ng) at 42°C overnight. Prior to detection, sections were incubated in 20ug/ml RNase A (Roche Applied Science) before DIG-labeled transcripts were detected according to manufacturer's protocol (Roche Applied Science).

Cell Culture

Tissue culture medium and supplements were purchased from Invitrogen (Life Technologies). All culture media were supplemented with heat inactivated FBS (JRH Biosciences or Hyclone, Thermo Scientific). Primary calvarial osteoblast cultures were prepared from 3 day old FVB/N mice (n=30) based on a protocol previously described [Thomas et al., 2000]. Bone fragments underwent 3 sequential digests in 0.1% collagenase A (Roche Applied Science)/ 0.05% trypsin (CSL)/0.02% EDTA/PBS for 30 min then demineralization for 10 min in 4mM EDTA/PBS. Further cell release was obtained by incubation of fragments with 1mg/ml collagenase/PBS for 45 min. The latter two incubations were repeated to obtain a total of seven cell populations, which were pooled and seeded at $1x10^4$ cells/cm^2 in α-MEM with 10% FBS, 2mM L-glutamine, 2.2g/L NaHCO$_3$, 10mM β-glycerophosphate, 50mg/L ascorbic acid and 100U/ml penicillin/streptomycin. MC3T3-E1 sub-clone 14 (ATCC, Cat# CRL-2594, RRID:CVCL_5437) cells (MC3T3) and MC3T3 stable lines expressing *Enc1* shRNA were maintained in growth media (α-MEM with 10% FBS, 2mM L-glutamine and 20mM HEPES). shRNA production was induced in MC3T3 lines by treatment with 2µg/ml doxycycline (dox) which was replenished at each media change. For differentiation, cells were seeded at $0.7x10^4$ cells/cm^2 in growth media supplemented with 10mM β-glycerophosphate and 50mg/L ascorbic acid. All cells were cultured at 37°C and 5% CO$_2$.

Alizarin Red staining and Alkaline Phosphatase assay

MC3T3 culture mineralization was assessed by Alizarin staining; cultures were fixed in 10% paraformaldehyde/PBS and stained with 2% Alizarin Red S (pH 4.2) for 10 min. Images were collected on the Perfection V700 Photo scanner (Epson). Alizarin stain was subsequently eluted in 10% cetylpyridinium chloride for 1h and quantitated at 540nm. For alkaline phosphatase (ALP) staining, cultures were fixed in 4% paraformaldehyde/PBS for 5 minutes then enzymatic activity was detected using the Alkaline Phosphatase staining kit (Sigma Aldrich), and imaged as above.

RNA preparation and quantitative RT-PCR

Total RNA was extracted from osteoblastic cells using the TRIzol reagent (Invitrogen) and treated with DNase I using the DNA-free kit (Ambion). cDNA was synthesized using Superscript III reverse transcriptase (Invitrogen) and quantitative RT-PCR was performed using SYBR green and the Rotor-gene RG-3000, Rotor-gene RG-6000 (Corbett Life Science), ABI Prism 7900HT Sequence Detection System or ViiA7 Real-Time PCR System (Applied Biosystems; Life Technologies). Relative gene expression levels were quantified using the $2^{\wedge}(-\Delta\Delta CT)$ method with cyclophilin or β-actin as the housekeeping gene. Primer sequences are shown in Table 1.

Antibodies and immunoblotting

To assess protein levels in cells, total cellular protein was isolated in RIPA buffer (50mM Tris-HCl, pH8, 150mM NaCl, 1% NP-40, 0.5% sodium deoxycholate, 0.1% SDS). Total cell lysates were quantitated using BCA protein assay reagents (Thermo Scientific). Samples were resolved by electrophoresis in 4-12% NuPAGE gels (Invitrogen) and transferred to PVDF membranes (GE Healthcare). Membranes were probed with ENC1 antibody (Santa Cruz Biotechnology Cat# sc-135896 RRID:AB_2293504), and β-actin (Abcam Cat# ab8227, RRID:AB_2305186) was used as a loading control. Bound primary antibodies were detected by chemiluminescent detection of HRP-conjugated secondary antibodies (GE Healthcare) and results quantitated using Image J software.

Statistical Analysis

All data analyses were performed in the open source statistical environment R (http://www.R-project.org/). One- or Two-way ANOVA analyses were performed depending on the data set. Fisher's PLSD post hoc tests were executed on main effects. Data are graphed as mean ± SE. Comparisons are indicated in the figure legends. Significance values are represented: *P<0.05, **P<0.01, ***P<0.001; #P<0.05, ##P<0.01, ###P<0.001.

RESULTS

Enc1 is expressed in osteoblasts and osteocytes

The cellular pattern of *Enc1* expression in adult mouse distal femur was determined histologically. *Enc1* transcripts were localized in mature periosteal osteoblasts, osteocytes, articular and growth plate chondrocytes, and in cells of the perichondrial Groove of Ranvier (Fig. 1A). Osteoblastic *Enc1* expression was confirmed in differentiating primary mouse calvarial cultures and in differentiating cultures of the pre-osteoblastic MC3T3 cell line (Fig. 1B), where mRNA was detected throughout culture phases of pre-confluent proliferation, matrix formation and matrix mineralization. In both cell types there was a significant decrease (by one-way ANOVA; p<0.05) in expression compared with levels at day 2 (at all time-points except days 8, 21, 22 for primary cultures; and at all time-points for MC3T3 cells). As the *Enc1* primers used for transcriptional analysis did not distinguish between encoded isoforms, the ENC1 protein profile during MC3T3 differentiation was analyzed (Fig. 1C). Two isoforms of the ENC1 protein were observed throughout 21 days of osteoblastic culture, with estimated mass of 67kDa and 57kDa compared with protein standards as previously found in primary neurons [Kim et al., 1998]. At later differentiation days (from day 12 onward) there was significantly more full length isoform than 57kDa ENC1 (Fig. 1D).

Knockdown of the ENC1 isoforms has graded effects on MC3T3 mineralization

As *Enc1* was expressed throughout MC3T3 osteoblastic differentiation the effect of ENC1 knockdown during osteogenesis was investigated using a doxycycline-inducible shRNA knockdown approach [Brown et al., 2010]. MC3T3 lines inducibly expressing *Enc1* shRNA were prepared as described in the Supplementary data and validated (Suppl. Fig.1). These lines express shRNA targeted to inhibit production of 67kDa ENC1 (line A) or shRNA targeted to inhibit both 57kDa and 67kDa ENC1 products (line B, C, D), in addition to a scrambled GFP (scGFP) control. The studies reported in this paper focused on ENC1 shRNA A and C lines.

In the absence of doxycycline, all cell lines exhibited comparable mineralization at differentiation day 21, the experimental endpoint (Fig 2A; column 1). With continuous induction of shRNA from Day 0 of differentiation, there was a striking increase in mineralization of the shRNA A line cultures compared with untreated controls (Fig. 2A; compare columns 1 and 2), confirmed by quantitation of eluted Alizarin Red staining (Fig. 2B). In contrast, under the same conditions there was an almost complete inhibition of mineralization in cultures of the shRNA C line, and in the two independent cell lines prepared using shRNA B and D sequences (Suppl. Fig. 2) that also knock down both 57kDa/67kDa ENC1 (Suppl. Table 2; Suppl. Fig 1). A modest increase in culture mineralization with expression of the scGFP shRNA sequence was presumably due to off target effects, as this control shRNA had no effect on Enc1 mRNA and protein levels (Suppl. Fig. 1).

To map the stage of differentiation when these ENC1 knockdown effects occurred, shRNA production was induced at later stages of osteogenesis (D5, 9, 13 and 18; Fig 2A, columns 3-6). Enhanced mineralized nodule formation in the shRNA A cultures was still observed with delayed induction of dox treatment at day 5 or 9, however induction at day 13 or later failed to show an effect of this shRNA on osteoblast differentiation. A significant inhibitory effect of shRNA C on mineralized nodule formation

persisted with delayed induction out to day 13, but was lost with shRNA induction at day 18. The level of mineralization in the shRNA A and C cell lines was significantly increased or decreased respectively, compared with the scGFP line, after multiple timepoints of induction (A, dox D0, 5; C, dox D0, 5, 9, 13). Doxycycline treatment at any day had little effect on mineralized nodule formation by the parental MC3T3 line.

Transient expression of ENC1 isoforms alters MC3T3 mineralization
As another test of the contribution of the ENC1 isoforms on MC3T3 differentiation, these cells were transiently transfected, on day 1, with ENC1 expression vectors encoding either 57 or 67kDa forms of the protein (cloned as described in the Supplementary data) or the pcDNA5/FRT/TO vector control. When cells were transfected with p57, there were significantly more Alizarin Red stained nodules at day 21 compared to cells expressing the p67 protein (Fig. 3A). The area of mineralization was likewise increased in the cells transfected with p57 compared with p67 ENC1 (Fig. 3B). Additionally, mineralization was significantly lower in the cells expressing p67 compared to cells transfected with the empty vector control.

Knockdown of ENC1 changes *Alpl* expression and ALP enzymatic activity levels
To further investigate the effect of ENC1 knockdown on MC3T3 differentiation, ALP activity was assessed (Fig. 4A). There was stronger ALP staining in cultures with induction of shRNA A compared to levels seen in both the MC3T3 parental cells and those expressing shRNA C, which mirrored enhanced mineralization results, and was evident as early as D6 of differentiation. In contrast there was an almost complete inhibition of ALP staining at all time-points assessed in shRNA C expressing cells. Levels of *Alpl* transcripts were consistent with the ALP staining pattern, with significant main effects of cell line, differentiation day and interaction (Fig. 4B).

Knockdown of ENC1 isoforms coordinately affects osteoblastic gene expression
Expression of osteoblastic genes was assessed in the shRNA lines at the stages of MC3T3 culture confluence (D3) and onset of mineralization (D13). After 3 days of differentiation, ENC1 knockdown had no effect on transcript levels for osteoblast marker genes *Runx2* (runt related transcription factor 2) and *Col1a1* (collagen, type 1, alpha 1); however, knockdown of both ENC1 isoforms in the shRNA C line led to decreased expression of osterix (*Sp7*) and *Ibsp* (integrin- binding sialoprotein) compared to the scGFP control (Fig. 4A). At this time point, knockdown of 67kDa ENC1 in the shRNA A cells resulted in increased expression of osteocalcin (*Bglap2*) but no other marker gene expression changes. At D13 the levels of *Sp7* and *Bglap2* transcripts were reduced with knockdown of both ENC1 isoforms in the shRNA C expressing cells, and there was a decline in *Ibsp* expression that did not reach statistical significance. As at D3, there was increased *Bglap2* in the shRNA A cell line, but there was also an increase in *Runx2*, *Sp7* and *Ibsp* levels at D13, unlike the earlier time point.

As there were striking effects of ENC1 knockdown on MC3T3 mineralization, genes involved in phosphate biochemistry were next assessed (Fig. 5B). At D3 in the shRNA C cells, there was decreased expression of *Alpl* and *Phospho1* (phosphatase, orphan 1), and increased expression of *Ank* (progressive ankylosis), *Enpp1* (ectonucleotide pyrophosphatase/phosphodiesterase 1) and osteopontin (*Spp1*) compared to the scGFP control. Conversely, there was an increase in *Alpl* expression with targeted knockdown of 67kDa ENC1 at this early timepoint, although the other genes involved in phosphate biochemistry tested here were not affected by this selective interference. At the onset of mineralization at D13, there were decreased levels of *Phospho1* transcripts in cells producing shRNA C and a trend for a decrease in *Alpl* expression (p=0.08), as was seen at D3. In the shRNA A cultures the expression levels of these two genes were increased, as were levels of *Enpp1* and *Spp1* transcripts. No changes in *Ank* mRNA levels were seen at this time point.

Expression of genes involved in *Wnt* pathway signaling were also investigated. At D3 there was increased expression of *Jun* (jun proto-oncogene) and decreased levels of *Dkk3* (dickkopf WNT signaling pathway inhibitor 3) in cells expressing the shRNA C compared to the control scGFP cells. There was also decreased expression of *Dkk3* with selective knockdown of 67kDa ENC1 at this time. There was significantly greater expression of *Jun*, *Fosl1* (fos-like antigen 1) and *Dkk2* (dickkopf WNT signaling pathway inhibitor 2) in the shRNA C cells compared with the shRNA A cells at this early time point. At D13, levels of *Axin2*, *Jun* and *Sfrp2* (secreted frizzled-related protein 2) were decreased, and *Frzb* mRNA was increased with targeted knockdown of 67kDa ENC1. Furthermore, *Myc* (myelocytomatosis oncogene) mRNA was lower, and *Jun*, *Sfrp2* and *Dkk2* were higher in the shRNA C cells. Expression levels of *Axin2*, *Myc*, *Sfrp2*, *Frzb* and *Dkk2* mRNA were significantly different between the shRNA A and C lines at this time point.

DISCUSSION

While the broad concepts underlying osteoblast differentiation are well understood, details clarifying the complexities of osteogenesis continue to emerge. As ENC1 was important in the differentiation of other cell lineages including closely related adipocytic cells [Kim et al., 1998; Zhao et al., 2000], we have analyzed the possible role of ENC1 in osteoblasts using an inducible-knockdown approach *in vitro* after confirming *Enc1* expression in mouse bone by *in situ* hybridization. We obtained histological and functional evidence supporting a regulatory role for ENC1 in osteoblast differentiation. In addition, we identified distinct osteoblastic mineralization patterns *in vitro* with differential knockdown of 67kDa ENC1 alone, or of 67kDa and 57kDa ENC1 together, for the first time revealing functional differences for the two ENC1 protein isoforms.

While there was a marked increase in MC3T3 mineralization with knockdown of 67kDa ENC1 and a striking decrease with knockdown of both ENC1 isoforms, there was no change in expression of the master osteoblastic transcription factor *Runx2* at culture confluence. However, there was reduced expression of the regulatory gene *Sp7* and the bone matrix component *Ibsp* at early stages after knockdown of both ENC1 isoforms, suggesting that although ENC1 may not act at the level of osteoblast commitment (i.e. through *Runx2* expression), it may regulate the progress of osteoblast differentiation. Both *Ibsp* [Li et al., 2010] and *Sp7* [Nishio et al., 2006] are RUNX2 target genes, and as RUNX2 is subject to phosphorylation [Li et al., 2016] and other post translational modifications [Jonason et al., 2009] that affect protein stability and transcriptional activity, these reduced mRNA levels early in MC3T3 differentiation, may reflect an effect of ENC1 knockdown on RUNX2 activity that remains to be elucidated.

Knockdown of ENC1 also had an early and coordinated effect on the expression of genes involved in phosphate metabolism and transport. Osteoblast mineralization is initiated in an orchestrated process involving an extracellular balance of available inorganic phosphate (Pi) which is a mineralization substrate, and pyrophosphate (PPi), an inhibitor of calcification. PPi is generated by the membrane glycoprotein ENPP1 [Johnson et al., 1999], exported from the cell by membrane transporter ANK [Ho et al., 2000], and converted into Pi in the extracellular space by ALPL [Johnson et al., 2000]. PHOSPHO1 also generates Pi in a non-redundant process, with the hydrolysis of phosphoethanolamine and phosphocholine in matrix vesicles [Yadav et al., 2011]. Maintenance of a physiological level of extracellular PPi is also important to prevent pathologic calcification of un-mineralized tissues including cartilage and vascular cells [Ho et al., 2000; Huang et al., 2008; Orimo, 2010].

With our knockdown of both 67kDa and 57kDa ENC1 in the shRNA C line we saw decreased expression of *Alpl* and *Phospho1* in early osteoblastic differentiation along with marked increases in expression of *Ank* and *Enpp1*. This set of expression changes suggest a mechanism for the failure of these cells to mineralize by increasing extracellular PPi levels and reducing available Pi. In these shRNA C cells, we

also saw increased expression of the extracellular matrix protein OPN, which directly binds to and inhibits the growth of mineralized crystals [Addison et al., 2007; Wada et al., 1999]. PPi treatment of MC3T3 cells can increase *Opn* expression [Addison et al., 2007], providing further support for a disruption of phosphate homeostasis in our shRNA C cultures. Conversely, increased ALPL levels at this early time point may help to explain the increased mineralization phenotype observed in the shRNA A cell cultures with targeted knockdown of only 67kDa ENC1. Our delayed induction of shRNA expression during the process of MC3T3 differentiation suggested that the window of vulnerability of these cells to ENC1 knockdown appears to close around the time of mineralization detection. As it has previously been demonstrated that alterations of PPi/Pi levels in early osteoblast cultures result in modulated downstream responses in mineralizing cultures through temporally regulated transcriptional and signaling events [Camalier et al., 2013], our observed early changes in expression of genes involved in PPi/Pi generation suggest a likely mechanism for the MC3T3 mineralization phenotypes that appeared as a result of ENC1 knockdown.

Alterations in early regulation of canonical Wnt/β-catenin signaling as a result of ENC1 knockdown appear mixed. The increase in expression of *Jun* and *Fosl1* target genes in the C line suggests that canonical Wnt pathways may be more in play in this cell line compared with cells expressing shRNA A. In our studies and those of others canonical Wnt signaling has an inhibitory effect on differentiation of MC3T3 and other osteoblastic cells (data not shown; [Eijken et al., 2008; Shi et al., 2007; van der Horst et al., 2005]), so increased expression of these canonical Wnt targets may feed into our observed low mineralization phenotype in this cell line. This up-regulation of canonical targets did not however extend to genes such as *Cdnd1* and *Myc* involved in cell cycle regulation. Consistently, we did not see any effect of ENC1 knockdown on cell proliferation (data not shown). *Dkk2*, though not a widely reported canonical Wnt target gene, has been found to be upregulated in MC3T3 cells upon treatment with canonical WNT1 [Li et al., 2005] and was also markedly upregulated in the shRNA C expressing cells. Interestingly, on the other side of the coin, in the cells with targeted knockdown of 67kDa ENC1 there was a marked increase in *Frzb* expression at D13. Treatment with FRZB has been shown to enhance osteoblast differentiation [Chung et al., 2004], and stable overexpression of FRZB in MC3T3 cells resulted in increased osteogenesis together with reduced canonical and increased non-canonical Wnt signaling [Thysen et al., 2016]. Concurrent decreases in expression of canonical Wnt signaling target genes *Axin2* and *Jun* suggest that a switch from canonical to non-canonical Wnt signaling in cells with targeted 67kDa ENC1 knockdown may be contributing to the enhanced mineralization phenotype that we see in these cells. The opposing patterns of expression of these genes involved in Wnt signaling in the A and C cell lines is compelling and warrants future investigation to determine the effect of the ENC1 isoforms in both canonical and non-canonical Wnt signaling pathways during MC3T3 differentiation.

The inhibition of MC3T3 cell differentiation with general knockdown of both ENC1 isoforms is consistent with previous studies in neuronal [Kim et al., 1998] and adipocyte [Zhao et al., 2000] cell lineages and suggests that regulatory mechanisms affected by ENC1 may be similar in diverse cellular contexts. A possible mechanism by which ENC1 might control differentiation of non-osseous as well as osteoblastic lineages could be through regulation of *Alpl* expression. ALP activity was increased during adipocyte differentiation and ALPL enzyme inhibition prevented lipid accumulation in 3T3-L1 cells [Ali et al., 2005]. In addition, ALPL has been found to be required for axonal growth in primary hippocampal neurons [Diez-Zaera et al., 2011]. As ALPL is essential in early stages of skeletal mineralization [Millan, 2013], the early dysregulation of the *Alpl* gene in the ENC1 knockdown MC3T3 cell lines may be a driver of the observed phosphate gene-related expression and mineralization phenotypes. In this context it is noteworthy that overexpression of 67kDa ENC1 in the HT29 colon cancer cell line had an inhibitory effect on ALP activity and caused a corresponding decrease in cellular differentiation [Fujita et al., 2001]. Although mechanistic aspects of these effects remain to be determined, the consistency of ENC1 overexpression and knockdown phenotypes reinforces the concept that any alteration in ENC1 level and isoforms may significantly alter cell physiology in multiple lineages.

Several limitations should be considered when interpreting the findings of this study. First, interpretation of the 57kDa ENC1 isoform knockdown is confounded by coordinate knockdown of the full length 67kDa isoform. While there was a reversal of the mineralization phenotype when 57kDa or 67kDa ENC1 isoforms were transiently transfected into MC3T3 cells, lending credence to the idea that the mineralization effects seen with shRNA C expression are due to a knockdown of the 57kDa ENC1 isoform, a conclusion that inhibition of MC3T3 mineralization and associated dysregulation of phosphate biochemistry was specifically due to altered 57kDa ENC1 here can only be inferred at this point. Secondly, while changes in the transcription of phosphate involved genes in cells by knockdown of the ENC1 isoforms are suggestive of an effect of these proteins on the maintenance of phosphate levels, an assessment and investigation of extracellular levels of PPi/Pi will be necessary to directly tie mineralization phenotypes to the changes in gene expression in the ENC1 knockdown lines reported here. Finally, confirming potential interactions of the ENC1 isoforms with canonical and non-canonical Wnt signaling mechanisms, especially in the context of expression of genes involved in phosphate regulation, would significantly add to understanding of the control of osteoblast mineralization.

In summary, here we have presented an initial study exploring the effects of the ENC1 isoforms on osteoblast differentiation. Our data indicate that the ENC1 gene is expressed and produces two protein isoforms throughout osteoblast differentiation. Differential knockdown of these two isoforms suggests that they have opposing roles in the process, modulating the expression of *Alpl* and other genes important in cellular phosphate homeostasis and osteoblast mineralization.

CONFLICT OF INTEREST

The authors declare that they have no conflicts of interest with the contents of this article.

ACKNOWLEDGEMENTS

REFERENCES

Addison WN, Azari F, Sorensen ES, Kaartinen MT, McKee MD. 2007. Pyrophosphate inhibits mineralization of osteoblast cultures by binding to mineral, up-regulating osteopontin, and inhibiting alkaline phosphatase activity. J Biol Chem 282:15872-83.

Ali AT, Penny CB, Paiker JE, van Niekerk C, Smit A, Ferris WF, Crowther NJ. 2005. Alkaline phosphatase is involved in the control of adipogenesis in the murine preadipocyte cell line, 3T3-L1. Clin Chim Acta 354:101-9.

Angers S, Thorpe CJ, Biechele TL, Goldenberg SJ, Zheng N, MacCoss MJ, Moon RT. 2006. The KLHL12-Cullin-3 ubiquitin ligase negatively regulates the Wnt-beta-catenin pathway by targeting Dishevelled for degradation. Nat Cell Biol 8:348-57.

Brown CY, Sadlon T, Gargett T, Melville E, Zhang R, Drabsch Y, Ling M, Strathdee CA, Gonda TJ, Barry SC. 2010. Robust, reversible gene knockdown using a single lentiviral short hairpin RNA vector. Human Gene Therapy 21:1005-17.

Camalier CE, Yi M, Yu LR, Hood BL, Conrads KA, Lee YJ, Lin Y, Garneys LM, Bouloux GF, Young MR, Veenstra TD, Stephens RM, Colburn NH, Conrads TP, Beck GR, Jr. 2013. An integrated understanding of the physiological response to elevated extracellular phosphate. J Cell Physiol 228:1536-50.

Choi J, Yang ES, Cha K, Whang J, Choi WJ, Avraham S, Kim TA. 2014. The Nuclear Matrix Protein, NRP/B, Acts as a Transcriptional Repressor of E2F-mediated Transcriptional Activity. J Cancer Prev 19:187-98.

Chung YS, Baylink DJ, Srivastava AK, Amaar Y, Tapia B, Kasukawa Y, Mohan S. 2004. Effects of secreted frizzled-related protein 3 on osteoblasts in vitro. Journal of Bone and Mineral Research 19:1395-402.

Diez-Zaera M, Diaz-Hernandez JI, Hernandez-Alvarez E, Zimmermann H, Diaz-Hernandez M, Miras-Portugal MT. 2011. Tissue-nonspecific alkaline phosphatase promotes axonal growth of hippocampal neurons. Mol Biol Cell 22:1014-24.

Ding J, Liu JJ, Kowal AS, Nardine T, Bhattacharya P, Lee A, Yang Y. 2002. Microtubule-associated protein 1B: a neuronal binding partner for gigaxonin. J Cell Biol 158:427-33.

Eijken M, Meijer IM, Westbroek I, Koedam M, Chiba H, Uitterlinden AG, Pols HA, van Leeuwen JP. 2008. Wnt signaling acts and is regulated in a human osteoblast differentiation dependent manner. Journal of Cellular Biochemistry 104:568-79.

Fujita M, Furukawa Y, Tsunoda T, Tanaka T, Ogawa M, Nakamura Y. 2001. Up-regulation of the ectodermal-neural cortex 1 (ENC1) gene, a downstream target of the beta-catenin/T-cell factor complex, in colorectal carcinomas. Cancer Res 61:7722-6.

Hernandez MC, Andres-Barquin PJ, Holt I, Israel MA. 1998. Cloning of human ENC-1 and evaluation of its expression and regulation in nervous system tumors. Exp Cell Res 242:470-7.

Hernandez MC, Andres-Barquin PJ, Martinez S, Bulfone A, Rubenstein JL, Israel MA. 1997. ENC-1: a novel mammalian kelch-related gene specifically expressed in the nervous system encodes an actin-binding protein. J Neurosci 17:3038-51.

Ho AM, Johnson MD, Kingsley DM. 2000. Role of the mouse ank gene in control of tissue calcification and arthritis. Science 289:265-70.

Huang MS, Sage AP, Lu J, Demer LL, Tintut Y. 2008. Phosphate and pyrophosphate mediate PKA-induced vascular cell calcification. Biochem Biophys Res Commun 374:553-8.

Jiang S, Avraham HK, Park SY, Kim TA, Bu X, Seng S, Avraham S. 2005. Process elongation of oligodendrocytes is promoted by the Kelch-related actin-binding protein Mayven. J Neurochem 92:1191-203.

Johnson K, Moffa A, Chen Y, Pritzker K, Goding J, Terkeltaub R. 1999. Matrix vesicle plasma cell membrane glycoprotein-1 regulates mineralization by murine osteoblastic MC3T3 cells. J Bone Miner Res 14:883-92.

Johnson KA, Hessle L, Vaingankar S, Wennberg C, Mauro S, Narisawa S, Goding JW, Sano K, Millan JL, Terkeltaub R. 2000. Osteoblast tissue-nonspecific alkaline phosphatase antagonizes and regulates PC-1. Am J Physiol Regul Integr Comp Physiol 279:R1365-77.

Jonason JH, Xiao G, Zhang M, Xing L, Chen D. 2009. Post-translational Regulation of Runx2 in Bone and Cartilage. Journal of Dental Research 88:693-703.

Kang MI, Kobayashi A, Wakabayashi N, Kim SG, Yamamoto M. 2004. Scaffolding of Keap1 to the actin cytoskeleton controls the function of Nrf2 as key regulator of cytoprotective phase 2 genes. Proc Natl Acad Sci U S A 101:2046-51.

Kim SG, Jang SJ, Soh J, Lee K, Park JK, Chang WK, Park EW, Chun SY. 2009. Expression of ectodermal neural cortex 1 and its association with actin during the ovulatory process in the rat. Endocrinology 150:3800-6.

Kim TA, Lim J, Ota S, Raja S, Rogers R, Rivnay B, Avraham H, Avraham S. 1998. NRP/B, a novel nuclear matrix protein, associates with p110(RB) and is involved in neuronal differentiation. J Cell Biol 141:553-66.

Kobayashi A, Kang MI, Okawa H, Ohtsuji M, Zenke Y, Chiba T, Igarashi K, Yamamoto M. 2004. Oxidative stress sensor Keap1 functions as an adaptor for Cul3-based E3 ligase to regulate proteasomal degradation of Nrf2. Mol Cell Biol 24:7130-9.

Lee H, Ahn HH, Lee W, Oh Y, Choi H, Shim SM, Shin J, Jung YK. 2016. ENC1 Modulates the Aggregation and Neurotoxicity of Mutant Huntingtin Through p62 Under ER Stress. Molecular Neurobiology 53:6620-6634.

Li X, Liu P, Liu W, Maye P, Zhang J, Zhang Y, Hurley M, Guo C, Boskey A, Sun L, Harris SE, Rowe DW, Ke HZ, Wu D. 2005. Dkk2 has a role in terminal osteoblast differentiation and mineralized matrix formation. Nature Genetics 37:945-52.

Li Y, Ge C, Franceschi RT. 2010. Differentiation-dependent association of phosphorylated extracellular signal-regulated kinase with the chromatin of osteoblast-related genes. Journal of Bone and Mineral Research 25:154-63.

Li Y, Ge C, Franceschi RT. 2016. MAP Kinase-Dependent RUNX2 Phosphorylation Is Necessary for Epigenetic Modification of Chromatin During Osteoblast Differentiation. Journal of Cellular Physiology doi:10.1002/jcp.25517.

Liang XQ, Avraham HK, Jiang S, Avraham S. 2004. Genetic alterations of the NRP/B gene are associated with human brain tumors. Oncogene 23:5890-900.

Metzger T, Kleiss C, Sumara I. 2013. CUL3 and protein kinases: insights from PLK1/KLHL22 interaction. Cell Cycle 12:2291-6.

Millan JL. 2013. The role of phosphatases in the initiation of skeletal mineralization. Calcif Tissue Int 93:299-306.

Nishio Y, Dong Y, Paris M, O'Keefe RJ, Schwarz EM, Drissi H. 2006. Runx2-mediated regulation of the zinc finger Osterix/Sp7 gene. Gene 372:62-70.

Orimo H. 2010. The mechanism of mineralization and the role of alkaline phosphatase in health and disease. J Nippon Med Sch 77:4-12.

Prag S, Adams JC. 2003. Molecular phylogeny of the kelch-repeat superfamily reveals an expansion of BTB/kelch proteins in animals. BMC Bioinformatics 4:42.

Resch A, Xing Y, Modrek B, Gorlick M, Riley R, Lee C. 2004. Assessing the impact of alternative splicing on domain interactions in the human proteome. J Proteome Res 3:76-83.

Robinson DN, Cooley L. 1997. Drosophila kelch is an oligomeric ring canal actin organizer. J Cell Biol 138:799-810.

Salinas GD, Blair LA, Needleman LA, Gonzales JD, Chen Y, Li M, Singer JD, Marshall J. 2006. Actinfilin is a Cul3 substrate adaptor, linking GluR6 kainate receptor subunits to the ubiquitin-proteasome pathway. J Biol Chem 281:40164-73.

Seng S, Avraham HK, Birrane G, Jiang S, Avraham S. 2010. Nuclear matrix protein (NRP/B) modulates the nuclear factor (Erythroid-derived 2)-related 2 (NRF2)-dependent oxidative stress response. J Biol Chem 285:26190-8.

Seng S, Avraham HK, Jiang S, Yang S, Sekine M, Kimelman N, Li H, Avraham S. 2007. The nuclear matrix protein, NRP/B, enhances Nrf2-mediated oxidative stress responses in breast cancer cells. Cancer Res 67:8596-604.

Shah AD, Shoback D, Lewiecki EM. 2015. Sclerostin inhibition: a novel therapeutic approach in the treatment of osteoporosis. Int J Womens Health 7:565-80.

Shi YC, Worton L, Esteban L, Baldock P, Fong C, Eisman JA, Gardiner EM. 2007. Effects of continuous activation of vitamin D and Wnt response pathways on osteoblastic proliferation and differentiation. Bone 41:87-96.

Sims NA, White CP, Sunn KL, Thomas GP, Drummond ML, Morrison NA, Eisman JA, Gardiner EM. 1997. Human and murine osteocalcin gene expression: conserved tissue restricted expression and divergent responses to 1,25-dihydroxyvitamin D3 in vivo. Mol Endocrinol 11:1695-708.

Stogios PJ, Prive GG. 2004. The BACK domain in BTB-kelch proteins. Trends Biochem Sci 29:634-7.

Sun L, Pan J, Peng Y, Wu Y, Li J, Liu X, Qin Y, Bauman WA, Cardozo C, Zaidi M, Qin W. 2013. Anabolic steroids reduce spinal cord injury-related bone loss in rats associated with increased Wnt signaling. J Spinal Cord Med 36:616-22.

Thomas GP, Bourne A, Eisman JA, Gardiner EM. 2000. Species-divergent regulation of human and mouse osteocalcin genes by calciotropic hormones. Exp Cell Res 258:395-402.

Thysen S, Cailotto F, Lories R. 2016. Osteogenesis induced by frizzled-related protein (FRZB) is linked to the netrin-like domain. Laboratory Investigation 96:570-80.

van der Horst G, van der Werf SM, Farih-Sips H, van Bezooijen RL, Lowik CW, Karperien M. 2005. Downregulation of Wnt signaling by increased expression of Dickkopf-1 and -2 is a prerequisite for late-stage osteoblast differentiation of KS483 cells. J Bone Miner Res 20:1867-77.

Wada T, McKee MD, Steitz S, Giachelli CM. 1999. Calcification of vascular smooth muscle cell cultures: inhibition by osteopontin. Circ Res 84:166-78.

Yadav MC, Simao AM, Narisawa S, Huesa C, McKee MD, Farquharson C, Millan JL. 2011. Loss of skeletal mineralization by the simultaneous ablation of PHOSPHO1 and alkaline phosphatase function: a unified model of the mechanisms of initiation of skeletal calcification. J Bone Miner Res 26:286-97.

Zhang DD, Lo SC, Sun Z, Habib GM, Lieberman MW, Hannink M. 2005. Ubiquitination of Keap1, a BTB-Kelch substrate adaptor protein for Cul3, targets Keap1 for degradation by a proteasome-independent pathway. J Biol Chem 280:30091-9.

Zhao L, Gregoire F, Sul HS. 2000. Transient induction of ENC-1, a Kelch-related actin-binding protein, is required for adipocyte differentiation. J Biol Chem 275:16845-50.

FIGURE LEGENDS

Figure 1. *Enc1* is expressed in bone and during differentiation of osteoblastic cells. (A) *Enc1* transcripts were detected in periosteal osteoblasts and cortical osteocytes (a), articular (b) and growth plate (c) chondrocytes and in cells of the perichondrial Groove of Ranvier (d) by *in situ* hybridization of adult mouse distal femur sections. (B) *Enc1* transcripts (normalized to expression at day 2) were expressed throughout differentiation of primary calvarial osteoblasts (top panel) and MC3T3 osteoblastic cells (bottom panel). Cells were harvested for RNA preparation (n=2 or 3) at the days shown. Vertical dotted lines denote culture confluence and onset of mineralization. *Enc1* was detected throughout periods of pre-confluence (P), matrix formation (MF) and mineralization (MIN). (C) Two isoforms of the ENC1 protein were detected during MC3T3 differentiation by western blotting. Blot is representative of three replicate experiments. (D) ENC1 isoform bands were quantitated relative to β-actin using Image J software. Results for 67 and 57kDa isoforms are presented in grey and black respectively. [#]57kDa vs. 67kDa Enc1.

Figure 2. Knockdown of ENC1 isoforms alters MC3T3 cell differentiation. MC3T3 parental and cell lines inducibly expressing shRNA sequences A, C and scGFP were differentiated in the presence or absence of 2µg/µl dox. (A) Cells were cultured without dox treatment (column 1) or in the presence of dox from differentiation days as shown (columns 2-6). At D21 of differentiation all cultures were stained with Alizarin Red and (B) levels of eluted stain were spectrophotometrically quantitated (n=3). There were significant main effects of cell line and day of induction, and an interaction between these effects (p<0.001). Results are representative of two independent experiments. * vs. no dox; [#] vs. scGFP.

Figure 3. Transient expression of ENC1 isoforms alters MC3T3 mineralization. MC3T3 cells at D1 were transiently transfected with expression constructs encoding full-length (p67) or 57kDa (p57) ENC1 isoforms or the pcDNA5 empty vector. Cells were grown in differentiation media and stained with Alizarin Red on D21. Nodule number (A) and mineralization area (B) were quantitated using Image J software, and presented relative to signal seen in pcDNA5 transfected cells (dotted line). Results are combined from three independent experiments. * vs. p67; [#] vs. pcDNA5.
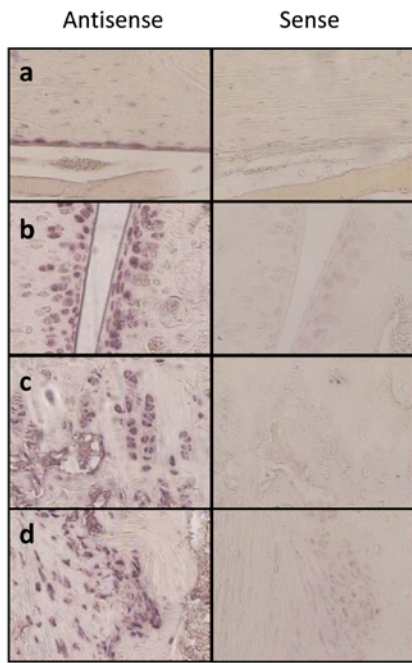
Figure 4. Knockdown of ENC1 isoforms alters alkaline phosphatase levels. MC3T3 parental cells and the stable cell lines induced to express shRNA sequences A, C and scGFP were differentiated in the presence of 2µg/µl dox. (A) At the time-points shown, cells were harvested and stained for ALP activity. (B) *Alpl* transcription was analyzed in the cell lines after differentiation for 3, 6 and 13 days (n=3). Levels were quantitated from shRNA A (blue, solid line), shRNA C (red, dotted line) and shRNA scGFP (green, dashed line) cells, relative to *β-actin* housekeeping gene. There were significant main effects of cell line and differentiation day, and an interaction between these effects (p<0.001). Results are representative of two independent experiments.

Figure 5. Knockdown of ENC1 isoforms alters gene expression. MC3T3 shRNA lines were differentiated in the presence of 2µg/µl dox to induce expression of shRNA sequences A, C and scGFP from day of plating. Expression of genes involved in Osteoblast differentiation (A), Phosphate biochemistry (B) and Wnt pathway signaling (C) were assessed at culture confluence (D3) and onset of mineralization (D13) (n=3), relative to *β-actin* housekeeping gene. mRNA levels in shRNA A (grey bars), and C (black bars) lines were normalized to levels seen in the scGFP line (dotted line). Data are representative of two independent experiments. [#]vs. scGFP control; * A vs. C shRNA line.
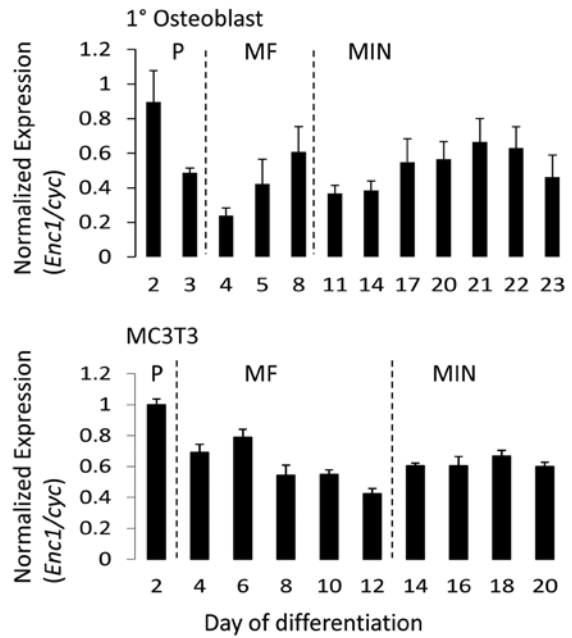
Table 1. Primer sequences used for qRT-PCR in MC3T3 cells

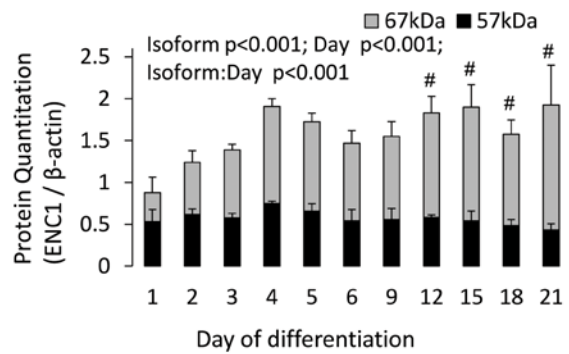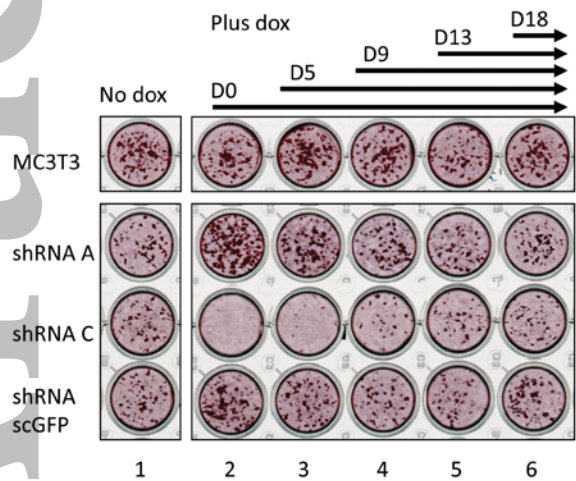| Target	Forward (5'→3')	Reverse (5'→3')
Enc1	CTGGTGTATGAGTCTGCGATGAAC	GCCTTGGGAATGATTTCTTTAGCC
Cyclophilin	GCCGATGACGAGCCCTTGGGCC	ACCAGTGCCATTATGGCGTGTG
β-actin	TCACCCACACTGTGCCCATCTACGA	CAGCGGAACCGCTCATTGCCAATGG
Alpl	GCCCTCTCCAAGACATATA	CCATGATCACGTCGATATCC
Runx2	AAGTGCGGTGCAAACTTTCT	TCTCGGTGGCTGGTAGTGA
Sp7	CCCTTCTCAAGCACCAATGG	AGGGTGGGTAGTCATTTGCATAG
Col1a1	AATGGCACGGCTGTGTGCGA	AACGGGTCCCCTTGGGCCTT
Ibsp	CGGTTTCCAGTCCAGGGAGGC	TTGGGCAGTTGGAGTGCCGC
Bglap2	CTCTGTCTCTCTGACCTCACAG	GGAGCTGCTGTGACATCCATAC
Phospho1	ACGGAGCAGAAGCACATCATC	TAGGCATCGTAGTCCAACAGC
Ank	TCATCCCCGACAGGAGCGGC	CCCACGGGGTAGGTGGCTGT
Enpp1	GTGGTACAAAGGACAGCCGA	CTGGTCCATGTGAATGCCCT
Spp1	TGCACCCAGATCCTATAGCC	CTCCATCGTCATCATCATCG
Axin2	CCTGACCAAACAGACGACGA	CACCTCTGCTGCCACAAAAC
Ccnd1	ACCCTGACACCAATCTCCTCAAC	TCTTCGCACTTCTGCTCCTCAC
Myc	GTCTTCCCCTACCCGCTC	CTGTCCAACTTGGCCCTC
Jun	TGAGTGACCGCGACTTTTCA	GAGGGCATCGTCGTAGAAGG
Fosl1	GCAAGTGGTTCAGCCCAAGAA	GTCCCAGGAAATGAGGCTGC
Sfrp2	GCCAGCCCGACTTCTCCTACAAG	CGGCAGGAGGTGGTCGCTACT
Frzb	ACATTCCAAGGGACACCGTC	CCGGGGATTAGAGTTCCTGC
Dkk2	CCGCTGCAATAATGGAATCT	GTAGGCATGGGTCTCCTTCA
Dkk3	GACACTCAGCACAAACTGCG	CCACCTGTCCACTCTGGTTG

Figure 1

Figure 2
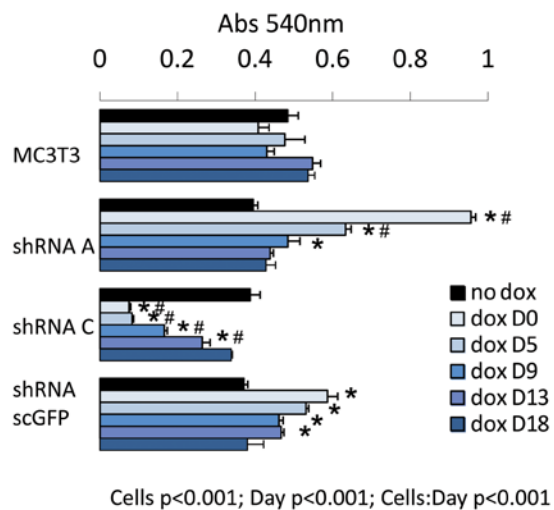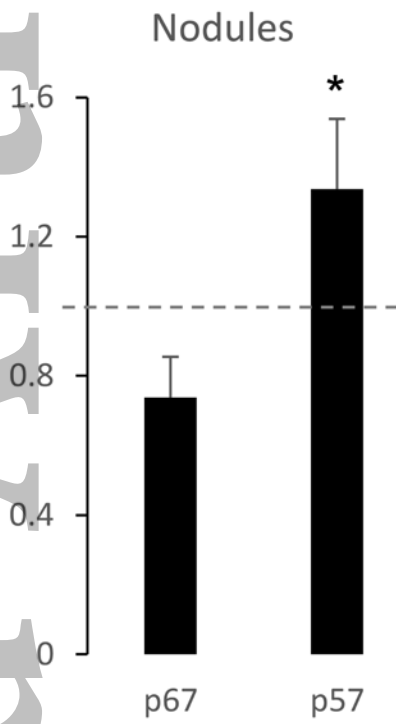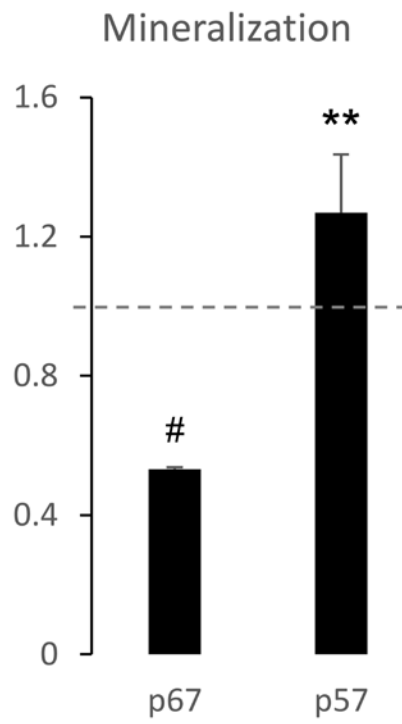
Figure 3

Figure 4

Figure 5